Polym Int 53:1397–1412 (2004)
DOI: 10.1002/pi.1587

Featured Article

Review of electronic and optical properties of semiconducting π-conjugated polymers: applications in optoelectronics

André Moliton[1]* and Roger C Hiorns[2]

[1]Unité de Microélectronique, Optoélectronique et Polymères, CNRS–FRE 2701, Faculté des Sciences et Techniques, 123 Av Albert Thomas, 87060 Limoges cedex, France
[2]Laboratoire de Physico-Chimie des Polymères, CNRS–UMR 5067, Hélioparc Pau-Pyrénées, 2 Avenue du Président Angot, 64053 Pau cedex 9, France

Abstract: A general overview of the optoelectronic properties of π-conjugated polymers is presented. Two types of polymer are discerned: interchangeable structures of the same energy (degenerate), such as polyacetylene; and non-degenerate polymers, such as poly(*para*-phenylene). The band structures of degenerate and non-degenerate polymers are related to their conductivities in doped and non-doped states. In both cases, disorder and impurities play an important role in conductivity. Polarons, bipolarons and excitons are detailed with respect to doping and charge transfers. Given the fibrillic nature of these materials, the variable range hopping (VRH) law for semiconducting polymers is modified to account for metallic behaviours. Optoelectronic properties—electroluminescence and photovoltaic activity—are explained in terms of HOMO and LUMO bands, polaron-exciton and charge movement over one or more molecules. The properties of H- or J-type aggregates and their effects on transitions are related to target applications. Device structures of polymer light-emitting diodes are explicitly linked to optimising polaron recombinations and overall quantum efficiencies. The particularly promising use of π-conjugated polymers in photovoltaic devices is discussed.

Keywords: π-conjugated polymers; electronic band structure; semiconducting and metallic behaviour; polymer light-emitting diode; polymer photovoltaic devices

INTRODUCTION

To prepare organic optoelectronic components, we will have to go beyond using passive materials such as insulators. The latter, such as polyethylene, are dielectric and display forbidden bands at energy levels ($\geq$5 eV) situated well outside the optical spectrum. The energy separation between molecular bonding (σ) and antibonding (σ^*) orbitals joining $-CH_2-$ groups is due to the considerable axial overlapping of these orbitals permitted by the polymer geometry. In contrast, the energy separation between π-bonding and π^*-antibonding orbitals is relatively small, as lateral orbitals exhibit limited overlapping. The band gap for polymeric solids containing such orbitals is typically between 1 and 3 eV, a value which covers the optical domain well. Furthermore, doping of such polymers gives rise to semiconducting materials, and the metallic state can be reached with certain materials such as polyaniline or its derivatives (Fig 1). It then becomes possible to envisage, for example, the fabrication of polymer light-emitting diodes (PLEDs) or photovoltaic cells.[1]

This is a review of particularly promising organic polymers which exhibit π-conjugation, often display high thermal stabilities, and are generally considered well apt to forming thin films over large surfaces, for example, by spin coating. Initially, the electronic structure of two types of π-conjugated polymer are presented. They are polyacetylene (PA),[2–4] which has a degenerate fundamental energy state due its access to two possible configurations, represented in Fig 2(a) and poly(*para*-phenylene) (PPP),[5] which is shown in Fig 2(b) and has a non-degenerate fundamental energy level. It should be noted that the widely used π-conjugated poly(*para*-phenylene vinylene) (PPV),[6] represented in Fig 3(b), is also non-degenerate. Secondly, we discuss the conducting properties of these polymers and, in particular, two types of behaviour: semiconducting and metallic. To form these electrical states, which will be detailed, the

* Correspondence to: André Moliton, Unité de Microélectronique, Optoélectronique et Polymères, CNRS–FRE 1072, Faculté des Sciences et Techniques, 123 Av Albert Thomas, 87060 Limoges cedex, France
E-mail: amoliton@unilim.fr
(*Received 24 November 2003; revised version received 2 February 2004; accepted 19 February 2004*)
Published online 19 July 2004

 Polym Int 0959–8103/2004/$30.00

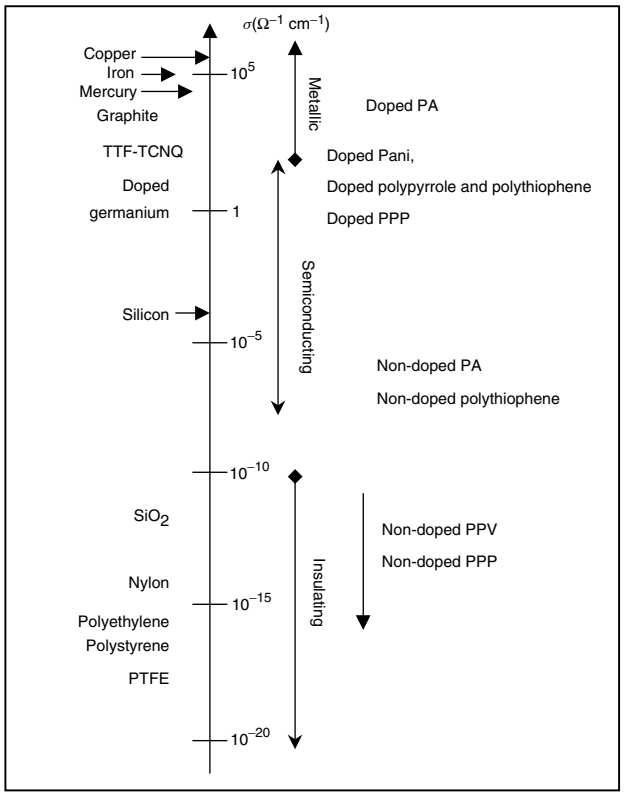

Figure 1. Conductivities of conjugated polymers compared with other common materials.

polymers need to be doped. Various types of doping may be used: (i) electrical doping by charge transfer from a donor (n-type) or acceptor (p-type) dopant to the organic solid; (ii) electric field effect doping in which an organic semiconductor or metal-insulator-semiconductor structure (MIS structure) is subject to positive or negative electrical polarisation due to influence from a grill with either n- or p-type dopants, respectively; (iii) unipolar injection of charges into an organic solid using an electrode; (iv) bipolar injection of opposed charges (electrons from cathode and holes from anode) which can generate certain quasi-particles, following migration through an organic solid; (v) optical doping associated with photogeneration of electron–hole pairs under the influence of light excitation; and (vi) doping–dedoping using acid–base equilibria (polyaniline (Pani) only) in a process

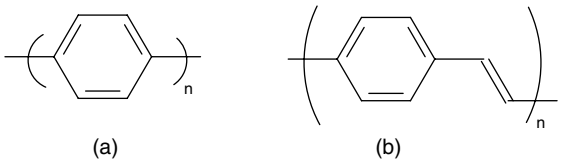

Figure 3. Structure of (a) PPP; and (b) PPV.

yielding metallic Pani with high conductivity ($\sigma > 200\,\Omega^{-1}\,cm^{-1}$).[7] Finally, two devices where π-conjugated polymers are used as alternatives to inorganic materials are presented. PLEDs have now been commercialised by Philips. Polymer solar cells, exhibiting yields of the order of 3 %,[8] have rapidly improved during recent years, so much so that researchers believe that these materials will provide a real alternative to expensive silicon-based cells in the near future.

ELECTRONIC STRUCTURE OF ORGANIC SOLIDS: IDEAL π-CONJUGATED POLYMERS

Degenerate π-conjugated polymers: PA, the archetypal 'conducting polymer'

PA was the starting point for research into conducting polymers at the end of the 1970s.[3,9] Each CH unit is linked by σ-bonds formed from three equivalent, triangular sp^2 hybrid orbitals, thus leaving a free fourth-orbital ($2p_z$) which is represented in Fig 4(a) by black dots. The backbone, with unit repetition a, can be considered one-dimensional relative to the $2p_z$ electrons. As detailed in Fig 4(b), for a chain of N carbon atoms, there are N p_z electrons which fill only half of the first band (which can contain $2N$ electrons), and therefore PA should behave as a metal (half-filled last band); however, this is not the case. To take this reality into account, we need to consider Peierls distortion[10] which gives rise to a dimerisation of the polymer backbone and an alternation of single and double bonds with repeat unit 2a, as schematised in Fig 5(a). The energy of deformation (E_{defor}) is less than the gain in electronic energy following the opening of a band gap (E_{relax}). The unchanged σ-orbitals maintain polymer rigidity. However, the permitted band can only take on N electrons, as its size has been halved (Fig 5(b)). Therefore, $N(p_z)$ electrons from N carbon

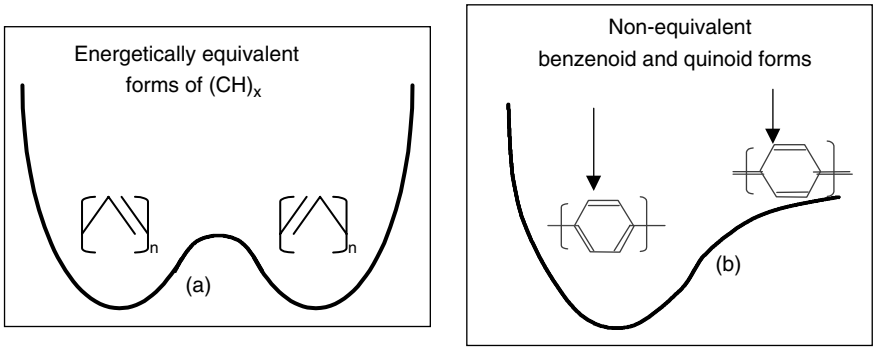

Figure 2. (a) Degenerate PA; and (b) non-degenerate PPP.

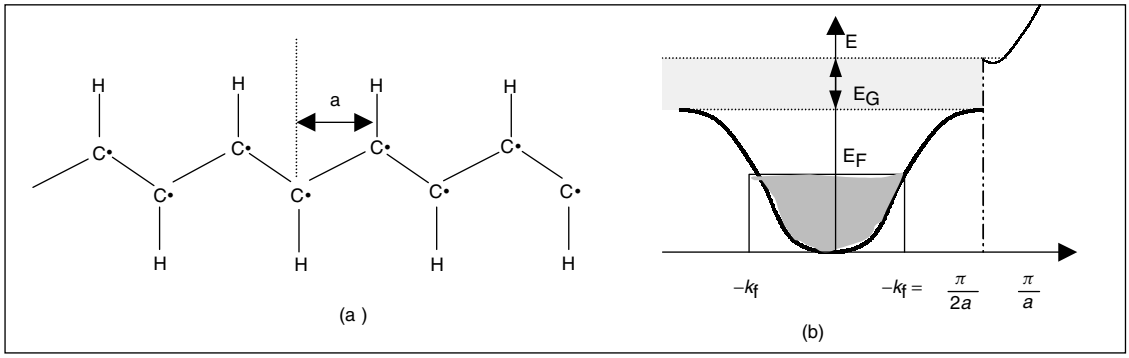

Figure 4. (a) Configuration of PA with repeat unit constant a; and (b) resulting band scheme corresponding to a weak bond approximation.

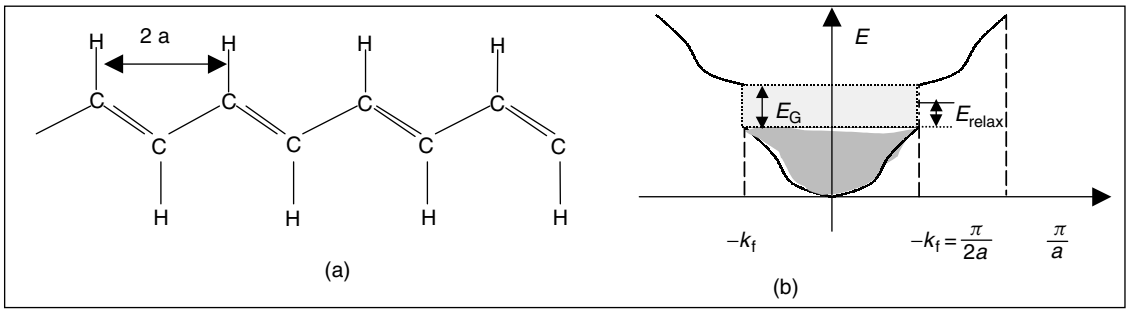

Figure 5. (a) Configuration of PA with period 2a; and (b) band scheme for this configuration.

atoms are trapped within this band. We can see that PA in its natural state is a semiconductor, with a band gap of the order of 1.5 eV.

Band scheme for a non-degenerate π-conjugated polymer: PPP

Assuming that PPP is based on a chain of benzene rings, we shall apply the Hückel theory to establish the form of the band scheme for an isolated polymer. We will then use techniques normally used for covalent, intramolecular bonds, which are appropriate for organic materials. Intermolecular interactions will not be considered in the initial stages. As mentioned above, overlapping between π-orbitals is weaker than that between σ-orbitals, and the separation between $\pi-\pi^*$ bonds is greater than that between $\sigma-\sigma^*$ bonds. We will thus be limited to studying π- and π^*-molecular orbital bands within which energy intervals are distributed in the highest occupied molecular orbitals (HOMO) and lowest unoccupied molecular orbitals (LUMO), otherwise termed bonding and antibonding states, respectively. Again respectively, these are analogues of valence (VB—the highest full band) and conduction (CB—the lowest empty or partially occupied) bands, which are traditionally presented in solid-state physics in a band scheme of weak bonds.[11]

Three steps are used to obtain a definitive band scheme: first, as simply as possible, the energy states of an isolated benzene ring (left side of Fig 6) are determined in one dimension using results obtained from Floquet's theorem;[12] second, (right side of Fig 6), the state interactions of a benzene ring within a polymer chain are brought into play resulting in a breakdown of π and π^* bands, due to molecular orbital coupling; and third, changes due to interactions between polymers are considered by using amorphous semiconductors as a model. A definitive band scheme can then be defined as in Fig 7.

Why conduction in HOMO or LUMO bands is not allowed

If we denote the height of large permitted bands as B ($B \gg kT$), an approximation of effective mass gives $m^* = \hbar^2/Ba^2Z$, in which Z is the co-ordination number. The mobility ($\mu = q\tau/m^*$ where q is the charge of an electron and τ is the relaxation time) of charge carriers within HOMO and LUMO bands in π-conjugated polymers can then be evaluated using $\mu = q\tau a^2/\hbar^2 B/Z$. In addition, and in accordance with the Ioffe and Regel condition,[13] for bands to retain a physical significance, B must be greater than ΔE ($\Delta E \approx \hbar/\tau$ Pauli principle). To enable conduction in these bands, the following must be true: $\mu = q\tau a^2/\hbar^2 B/Z > q\tau a^2/\hbar^2 \Delta E/Z \approx qa^2/\hbar 1/Z$.

The inequality, $\mu > qa^2/\hbar 1/Z$, is the final condition for conductivity in delocalised bands of size B. With a of the order of several angstroms, about the length of a strong bond in a π-conjugated polymer, and $Z \approx 2$, the resulting conduction is $\mu > 10^{-1}\,\mathrm{cm^2\,V^{-1}\,s^{-1}}$. As the observed value for these polymers is typically of the order $\mu > 10^{-4}\,\mathrm{cm^2\,V^{-1}\,s^{-1}}$, we can conclude that transport probably does not occur within these delocalised bands. We are therefore obliged to recognise that, in π-conjugated polymers, charge mobility is principally *via* other states.

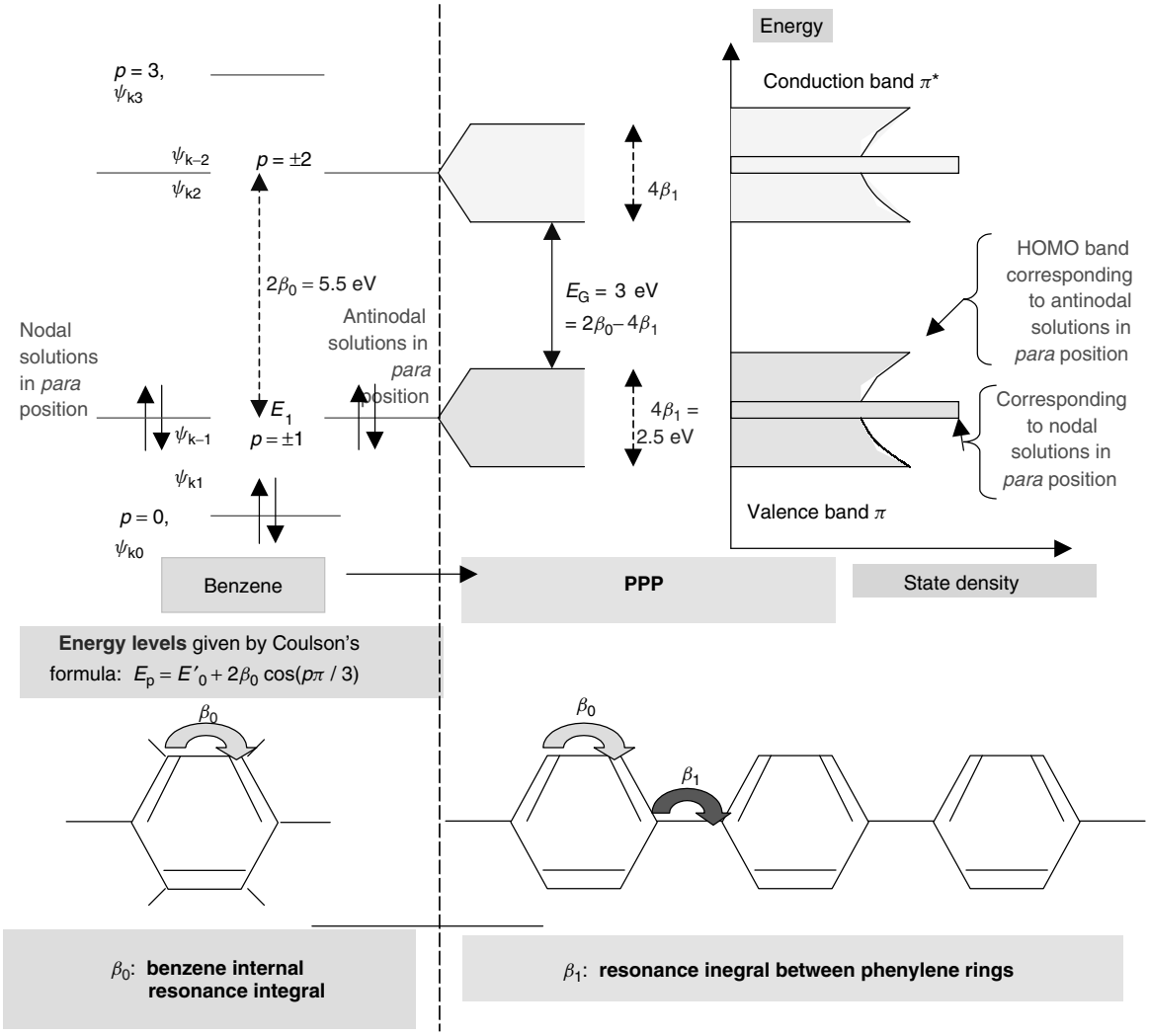

Figure 6. Schematisation of energy levels. On the left, benzene and on the right, PPP. Note that Ψ is the wavefunction at level k.

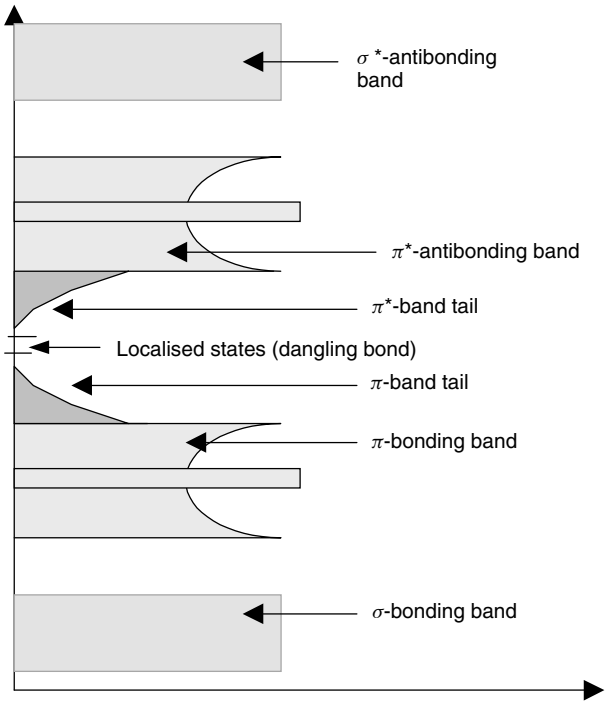

Figure 7. Band scheme for a π-conjugated polymer including affects due to 3-D interchain interactions.

ELECTRONIC BAND STRUCTURES OF 'REAL' CONJUGATED POLYMERS

Effects due to inter-chain interactions and disorder

It should be highlighted that the results obtained up to now have only dealt with intra-chain interactions in mono-dimensional models, and that inter-chain interactions, which appear once we reason in 3-D, will modify the results considerably, especially at the level of transport processes.[14] Inter-chain transfer integrals of around 0.1 eV have been obtained for PPV,[15] a polymer with a conjugation similar to that of PPP. The actual inter-chain mobilities, which clearly determine to a high degree the overall mobility of the material, are thus very much lower. In addition, a sample of PPP normally contains polymers with various conjugation lengths. With each increase in conjugation length, there is an increase in the distribution size of π and π^* states, situated at band edges, resulting in bathochromic effects. On applying results obtained from amorphous semiconductors,[9,16] these inter-chain effects remove the brutal discontinuity observed at the band edges of an isolated chain. In its place, there are band tails which resemble those of amorphous

semiconductors such as silicon. Forbidden states in the middle of the band can also be added to allow for dangling groups (chain ends, structural deformations), which can appear during thermal (*eg*, on synthesis) or radiation treatments. The resulting band scheme is shown in Fig 7.

An example of a structural defect can be given for the degenerate PA. As shown in Fig 8(a) PA is obtained in the *cis* form directly following synthesis, however, with increasing temperature it tends towards the *trans* form. During the isomerisation process, defects appear in the alternating double and single bonds. Defects can arise due to the chain being energetically equal on either side of a $-CH-$ unit, as two configurations can equally be formed, as shown in Fig 8(b). From an energetic point of view, the thus formed soliton state is equivalent to a dangling bond, with the lone electron in a $2p_z$ configuration. The state is midway between π- and π^*-levels, as shown in Fig 9(a). The Peierls distortion forms a band gap between the full and empty bands (Fig 9(b)) and the state density function where the soliton (or dangling bond) is situated in the middle of the gap (Fig 9(c)). Overall, the chain remains electrically neutral, with the carbon near the soliton being surrounded by four electrons, however, the system can give a paramagnetic signal due to the unmatched electron having $s = 1/2$.

The effect of excess charges on a polymer chain

Degenerate π-conjugated polymers

n-Type donors, such as alkali metals, can transfer an electron to PA. p-Type acceptors, such as I_2 or AsF_5, are capable of taking an electron from PA. Here we use the example of PA on which there are two solitons corresponding to two excited states. On doping the chain, one of the solitons is ionised to yield an associated pair of a charged soliton and a neutral anti-soliton. As the degree of doping increases to around 30 % w/w, an increasingly large soliton band appears which can close the forbidden band.[17]

Non-degenerate π-conjugated polymers and polaron states

If an electron is placed on a lattice, the resulting displacement of atoms reduces the electron's energy so that a potential well containing the electron is formed. If the well is deep enough, the electron will find itself in a tied state and is 'self-trapped'. As such, the electron and its associated lattice deformation is termed a 'polaron'.

Here PPP is used as an example.[17–19] In the neutral state, the stable structure of PPP is based on benzylic rings. Following doping, local reorganisation leads to a stable quinoid-based form of the polymer (Fig 10). Figure 11 details variations in energy with respect to geometric configuration and indicates how a chain based on quinoid units is stable in its ionised state (curve c). The energy due to chain distortion (E_{dist}) in going from the unstable ionised benzoic (curve d) to quinoid forms is more than compensated for by the gain in relaxation energy (E_{relax}).

Ionisation of the chain gives rise to polaron levels localised inside the forbidden band (Fig 12(c)), and on the right of Fig 12 we can see the evolution of energy levels on increasing the density of introduced charges (doping density) and of the Fermi level, which sits midway between the lowest unoccupied and the highest occupied levels. Ultimately the rise of the polaronic bands can fully occupy the HOMO and

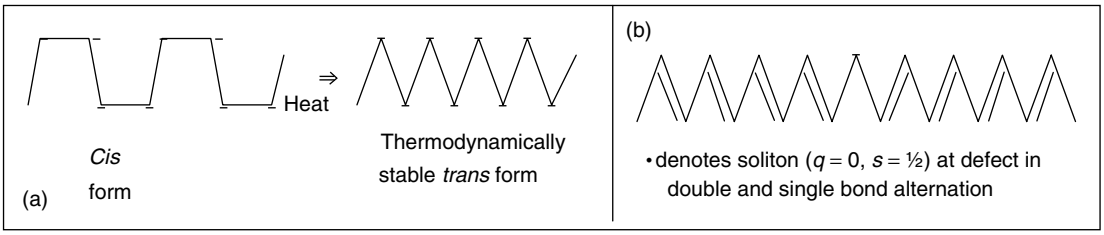

Figure 8. (a) *Cis–trans* isomerisation in PA; and (b) soliton-type defect in PA.

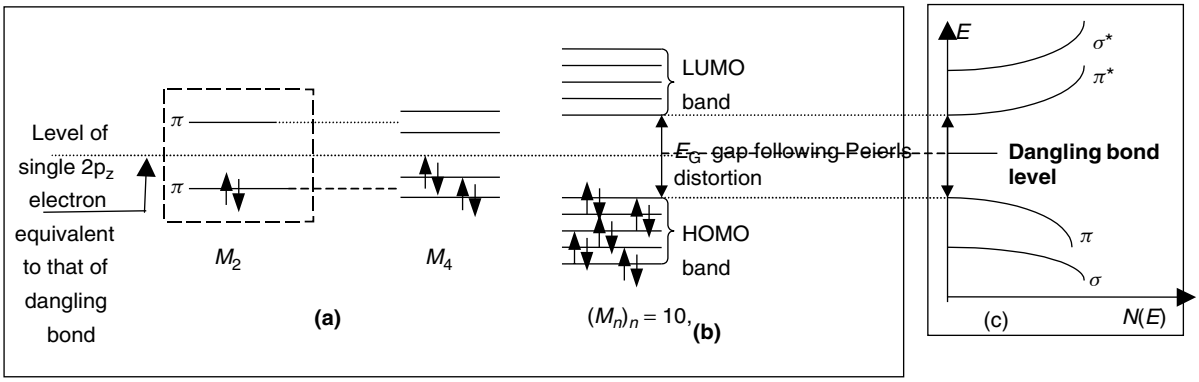

Figure 9. (a) Energy level evolution with increasing monomer (*M*) units, going from 2 to 4 and then to *n*; and (b) for a chain of *n* monomers, Peierls distortion gives rise to gap E_G; (c) resulting band scheme generated by Peierls distortion, also showing dangling bond level.

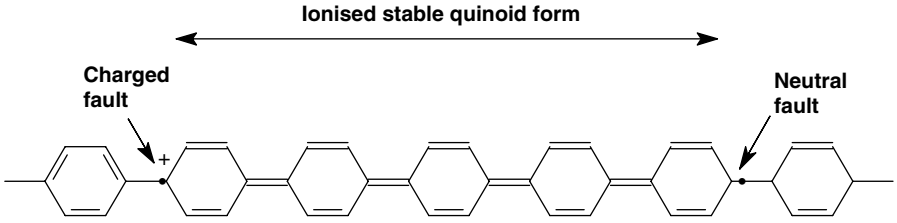

Figure 10. Representations of the once-ionised stable quinoid form of PPP.

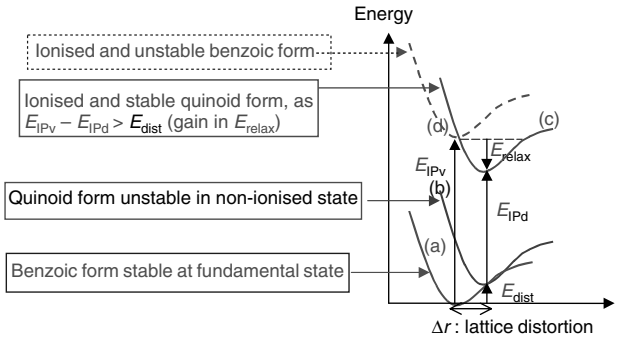

Figure 11. Configuration curves for PPP chains in neutral and ionised states, in which v and d denote vertical and distorted state transitions, respectively.

LUMO bands, and a metallic state cannot appear. Conductivity is then governed by hopping mechanisms between polaronic states.

Polyaniline

Pani forms a rich family of electronically active polymers. The free doublet electrons on the nitrogen atoms participate in the formation of orbitals delocalised along the polymer chain, as schematised in Fig 13(a).

The degree of disorder in Pani is highly sensitive to the method of preparation used, to the point where deviation from coplanarity of adjacent rings can be effected.[20] An acid–base equilibrium can be used to dope and dedope Pani (Figs 13(b)). The doped emeraldine salt is conducting because it exhibits a 'crystalline' structure.

TRANSPORT MECHANISMS

In terms of transport mechanisms, there are two main classes of polymers: semiconducting, such as PPP, and conducting, such as doped Pani.

Electrical conductivity of semiconducting polymers

Irrespective of polaronic states or states tied to localised defects, the variable range hopping (VRH) law may be qualitatively verified.[21] The VRH law is followed by a carrier with little thermal energy which is limited to hopping to energetically close levels, even though they may be spatially well separated. Thus the probability of transitions occurring due to tunnelling effects is diminished due to a large barrier. The VRH law does, however, take an optimisation of the hopping distance into account: $\sigma \propto \exp[-(T_0/T)^{\gamma}]$, with $\gamma = [1/(d+1)]$, ie, $\gamma = 1/4$ in 3-D, $\gamma = 1/3$ in 2-D, and $\gamma = 1/2$ in 1-D.

Various improvements of this law have been proposed. In order to account for the behaviour of π-conjugated polymers doped to varying degrees, Kaiser modelled a heterogeneous structure base on two domains (Fig 14).[22] Domain 1 consists of fibrils within a matrix of Domain 2, which act as an

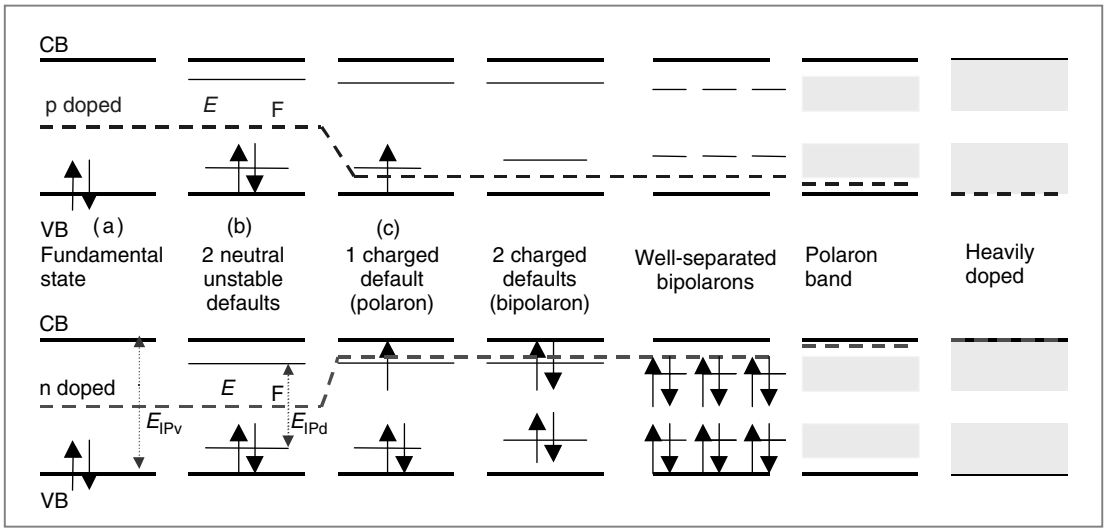

Figure 12. PPP and evolution of energy levels with p-doping (top) and n-doping (bottom).

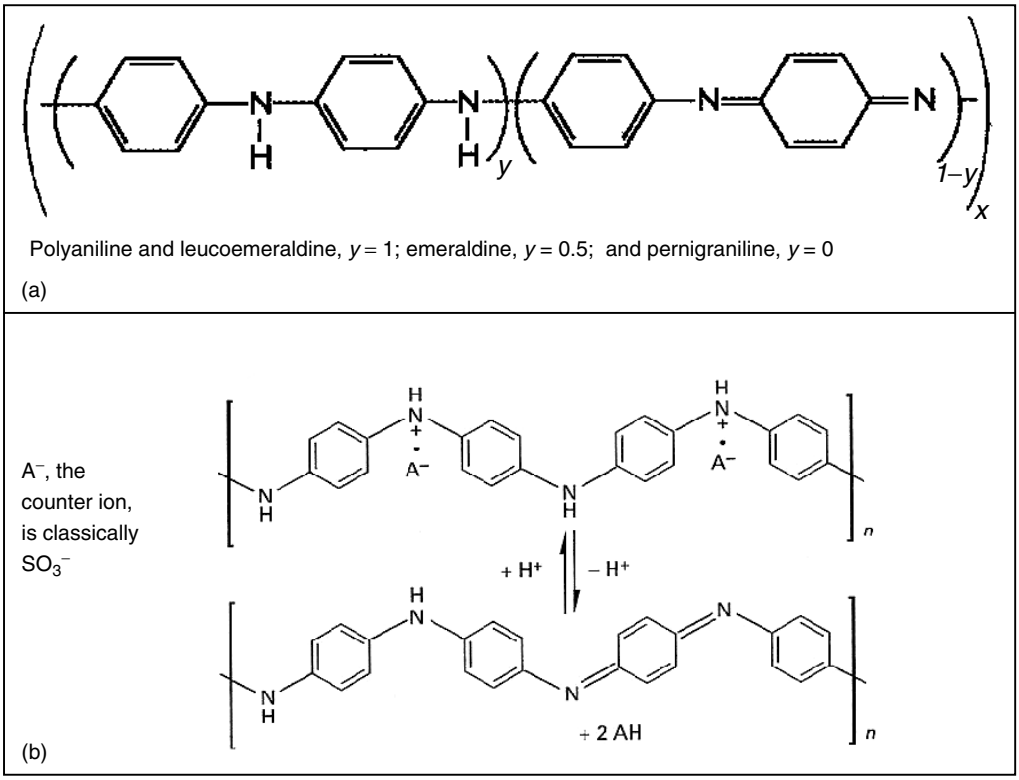

Figure 13. Pani structures.

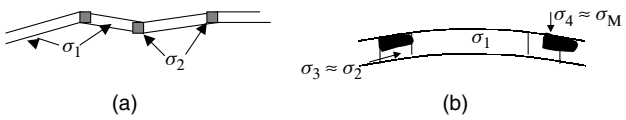

Figure 14. Heterogeneous systems in (a) semiconducting state; or (b) in a metallic state.

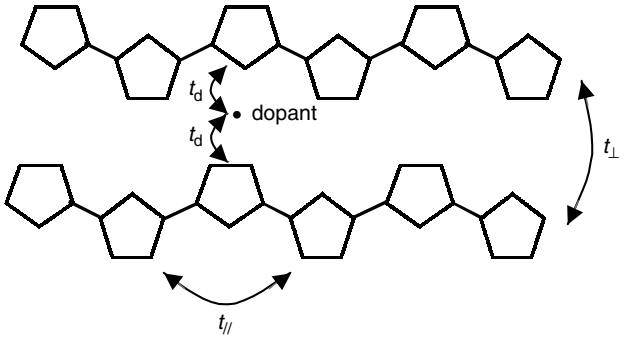

Figure 15. Representation of dopant bridging between two conjugated polymers showing transfer integrals.

electron barrier. The conductivity can be expressed as $\sigma^{-1} = f_1\sigma_1^{-1} + f_2\sigma_2^{-1}$, where f_i is a factor in the form $f_i = L_iA/pLA_i$ with p representing the number of conducting pathways given by the ratio L_i/A_i of sample length over cross-sectional area. When $\sigma_1 \gg \sigma_2$, due to the presence of sufficient dopants, we have $\sigma \approx f_2^{-1}\sigma_2$ and the evolution of σ is mostly guided by σ_2. This means that transport mechanisms assisted by tunnelling effects are dominant, and at low temperatures the hopping mechanism (VRH) proposed by Mott is relevant.[23] It should be noted that the value of σ can be high due to the term f_2^{-1}, which is proportional to L/L_2, where L is higher than L_2, the thin inter-fibril barrier.

Other models of isotropic conductivity, often observed in doped π-conjugated polymers, have been elaborated. Interchain charge transport is relatively facile due to the presence of a non-inconsequential overlapping between π-orbitals of adjacent chains. Electron transfer between chains is effected either by direct three-dimensional coupling or *via* intermediate doping ions. Figure 15 gives an example of a dopant ion between chains which can transfer a carrier with equal ease in either direction. On a small scale, when there is a high enough concentration of dopants to connect adjacent chains, then clusters of polarons resembling networks form. On a larger scale though, the polarons spread inhomogeneously in a disordered polymer network and the polaronic clusters are separated.

A calculation for conductivity by hopping for this configuration has been made using the following three hypotheses: (i) adiabatic hops occur within polaronic clusters; (ii) non-adiabatic hops occur between polaronic clusters, with the intervention of phonons; and (iii) electrostatic energy is the principal barrier in the hopping mechanism.[24]

The relationship found for conductivity is: $\sigma = \sigma_0 \exp\left[-(T_0/T)^{1/2}\right]$. T_0 depends on both the charge energy of clusters and system granularity such that $T_0 = 8U/k\left(\overline{\delta}/\delta - 1\right)^2 / \left(\overline{\delta}/\delta - 1/2\right)$ where $U = 1/4\pi\varepsilon_0\varepsilon_r e^2/a$ and represents electrostatic repulsion between two electrons separated by distance a,

δ is the mean distance between dopants in a cluster and is independent of cluster size, and $\overline{\delta}$ is the mean distance between dopants assuming a homogeneous distribution and ignoring clusters.

Conducting polymers

Initially, it was considered that these polymers exhibited a 'metallic' character (degenerate medium with the Fermi energy level (E_F) in delocalised states due to disorder). Conductivity parallel to the chain axis can be expressed using the Drude–Boltzmann relationship: $\sigma = \sigma// = nq^2 l/\hbar k_F$ in which l is the mean free path and q is the charge on an electron. Given that $k_F = \pi/a$, we obtain $\sigma// = \left(nq^2a^2/\pi\hbar\right)(l/a)$ (equation used by Kivelson and Heeger[25]). With respect to temperature: (i) at low temperatures, inelastic collisions are controlled by electron–electron interactions, with $l \propto T^{-1}$, resulting in $\sigma \propto T$ (Mott's linear law); and (ii) at higher temperatures, collisions with phonons dominate with $l \propto T^{-1/2}$, giving $\sigma \propto T^{1/2}$.

However, Kaiser's model appears more realistic.[22] At high levels of dopant, in order to account for a finite value for σ at temperatures tending to 0 K and the increase in thermoelectric power with T at low temperatures, the representation of the semiconducting state using fibrils needs to be modified. Thus two parallel domains are substituted for the second domain, the first of which (conductivity σ_3) continues to represent inter-fibril hopping, while the second introduces, like an amorphous metal, a supplementary component (σ_4) as if for an amorphous metal in the form $\sigma_4(T) = \sigma_{40} + \alpha T^{1/2}$, in which σ_{40} and α are constants. Overall, this gives

$$\sigma^{-1} = (f_1\sigma_1)^{-1} + (g_3\sigma_3 + g_4\sigma_4)^{-1}$$

where g_3 and g_4 are form factors.

Comparing metallic and semiconductor polymer behaviour

The conductivities of the two classes of polymers are summarised in Fig 16.

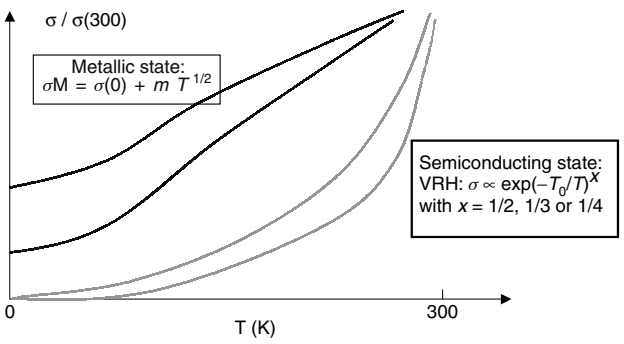

Figure 16. Change in conductivity of semiconducting and conducting polymers with temperature.

CHARGE GENERATION AND RECOMBINATION IN SEMICONDUCTING POLYMERS: OPTICAL PROPERTIES FOR ELECTROLUMINESCENT OR PHOTOVOLTAIC MECHANISMS

Excitons

So far we have detailed charge transport in chemically doped conjugated polymers in the presence of counter ions. An alternative method is that of carrier injection at both anode and cathode, which produces a double electrical charge injection. The result can be thought of as positive and negative polarons appearing at opposing electrodes, as shown in Figs 17(a) and 17(b).[1] On applying a potential field, each polaron migrates across the material until they meet, at which point they form an excited but neutral species. (The electron and the hole are excited outside of the HOMO and LUMO bands.) It is this species which is called a polaron-exciton and shown as a polaron-exciton singlet in Fig 17(c).

Using PPP as the example, Fig 18 represents the generation of an intra-chain polaron-exciton.[26] There is strong coupling between electron and vibrational excitations as each inserted charge results in a strong geometric distortion of the lattice, which displays a quinoid-based structure.

When a radiant combination occurs, photons with an energy higher than that which separates the energy levels of two polarons (or bipolarons) are often formed, which would indicate that lattice coupling, and any induced distortions, are smaller than those envisaged by previous models of polarons or bipolarons. The charges which make up the exciton, which is no longer a polaron-exciton, are thus tied to each other by an energy of no more than several tenths of an electronvolt. This can be due to several factors (which break any symmetry of the system Hamiltonians) which are subject to numerous controversies.[27] Furthermore, depending on the solid, the excited electron–hole pair can be localised on the same molecule (Frenkel exciton) or over different molecules (Wannier exciton).[28] Important effects can result when the excited molecules are close together (as in aggregates).

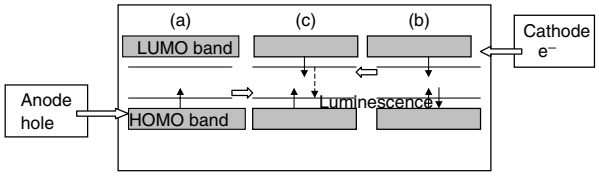

Figure 17. Electron–hole injection yielding a polaron-exciton.

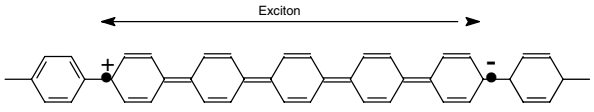

Figure 18. Representation of an intra-chain exciton in PPP.

Energy levels and transitions in coupled molecules (aggregates): consequences for electroluminescent and photovoltaic properties

For a 'top-to-bottom' orientation of two molecules, shown in Fig 19(a), the transitional momenta can be summed (momentum M_+ corresponding to energy E_+) to give an allowed transition (indicated by full arrow) or can zero each other out (momentum M_- corresponding to energy E_-) to yield a forbidden transition (indicated by the dashed arrow). A straightforward and seemingly reasonable result is obtained with a parallel molecule orientation, as shown in Fig 19(b).[1]

Transitions associated with optical absorption and spontaneous emission (fluorescence with non-delayed recombination of electron–hole pairs) are presented in Fig 20 for two separated and for two coupled molecules (which may occur in aggregates, for example). If the transitional moments of the two molecules are parallel to each other and perpendicular to their axis, as shown in Fig 20(a), it is the upper level which corresponds to the permitted transition and absorption, and accordingly there is a blue-shift. Transitions to the lower level are forbidden, so that, following relaxation from the higher to the lower level, any fluorescence is very weak and will penalise any electroluminescence. Effectively, the pair of molecules take on the 'H aggregate' co-ordination (the letter H resembles the geometric form). However, once the system is relaxed, the return from excited to fundamental states is improbable and the excitation (exciton) can diffuse over relatively long distances ($\approx$100 nm). This latter property can be of benefit to photovoltaic effects where the necessary separation of electrons and holes is favoured by the presence of an electric field.

Molecules at the centre of J aggregates (the letter J symbolises the bottom-to-head alignment of the molecules) are orientated so that it is the lower level that absorbs or emits (Fig 20(b)). This positioning of the molecules is beneficial to electroluminescence but penalises any photovoltaic properties. Excitons need only travel short distances before recombining, leaving little chance that they will meet an active centre such as a volume heterojunction, which could give rise to a potential difference permitting their separation.

In order to obtain fluorescence from solids, the parallel arrangement of molecular transition moments are preferred. H aggregates should be avoided, while J aggregates should be favoured (as they have linearly trained dipole moments). In photovoltaic systems, the inverse is true: J aggregates should be avoided and H aggregates should be favoured. This is because the former display low exciton diffusion lengths, while the latter aid the separation of holes and electrons. This explains the wide use of liquid-crystal-state polymers in photovoltaic research.[29]

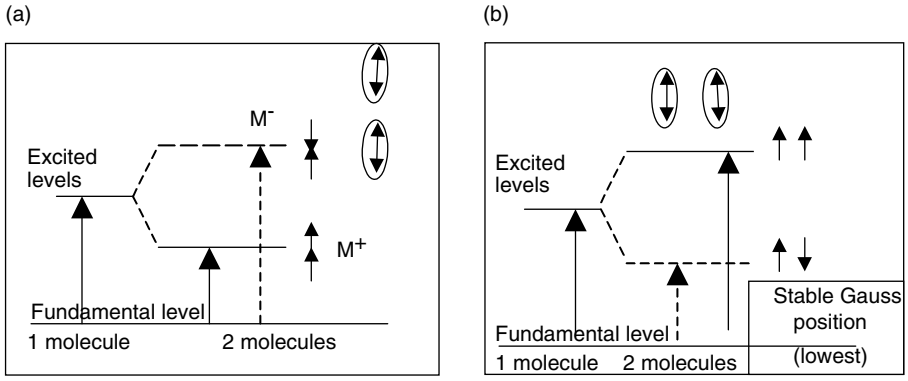

Figure 19. Classification of possible transitions for classic arrangements of two coupled molecules: (a) 'top-to-bottom' arrangement (red-shift); and (b) parallel arrangement (blue-shift).

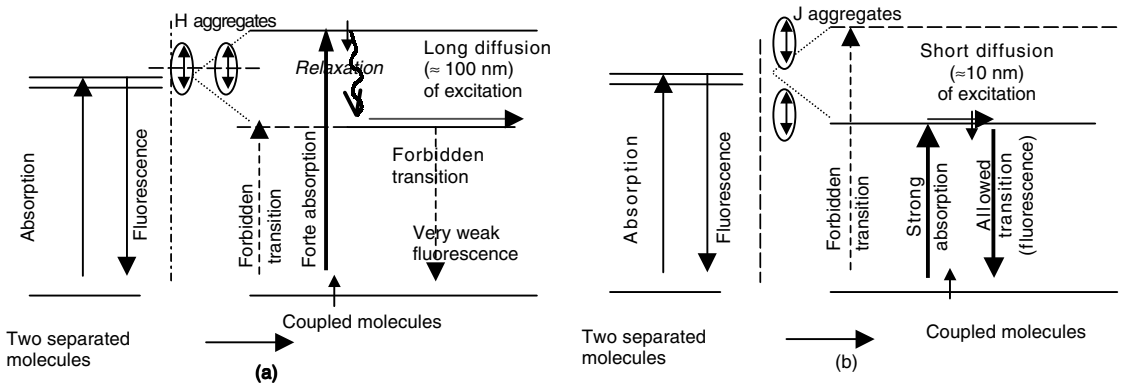

Figure 20. Transitions and excitation diffusions of (a) H aggregate; and (b) J aggregate.

ELECTROLUMINESCENCE OF π-CONJUGATED POLYMERS

The principal steps to electroluminescence

In general terms, the study of photometric characteristics of PLEDs, in particular their quantum yields and lifetimes, are guided by an understanding of the underlying mechanisms of charge behaviour and recombination (radiative or not) within organic materials. A typical organic light-emitting diode (OLED) structure is schematised in Fig 21, and it is very much different from that used for inorganic diodes. It is not possible to use organic semiconductors in their doped form, which would permit the fabrication of pn junctions similar to inorganic diodes, as doping agents tend to act as extinction centres, 'killing' radiative luminescence.[30,31] In organic materials, the low mobility of the charge carriers is exploited: when two charges are injected into the emissive layer and come into close proximity, their recombination is inevitable. This is in contrast to inorganic systems where charge carriers have such a high mobility that recombination centres are necessary. It is thus useful to study how organic diodes function in terms of four successive steps (Fig 22): (i) and (i′) injection of electrons and holes at the cathode and the anode, respectively; (ii) their transport through one or more organic layers; (iii) their association to form an exciton quasi-particle; and (iv) and (iv′) the relaxation of the quasi-particle resulting in luminescence and non-radiative emissions, respectively.

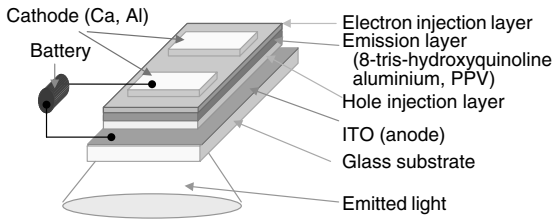

Figure 21. Typical structure of an electroluminescent organic diode.

Quantum efficiency and ways of improving PLEDs

The external quantum efficiency ($\eta_{\Phi ext}$) is defined by:[32]

$$\eta_{EL} = \eta_{\Phi ext} = \frac{\text{number of produced photons}}{\text{number of injected charges}}$$

$$= \eta_{opt}\eta_{\Phi int} \text{ where } \eta_{\Phi int} = \Phi_f \eta_r \gamma \text{ and } \eta_{opt} = \frac{1}{2n^2}.$$

The factor $1/2n^2$ for optical efficiency is introduced to account for refractions at the air–material interface. $\eta_{\Phi int}$ Is the internal quantum efficiency and consists of three factors. The first is the efficiency of recombination of injected carriers (γ) for which $\gamma = \mathcal{J}_r/\mathcal{J}_T$ where $\vec{\mathcal{J}}_T$ is the total current density and $\vec{\mathcal{J}}_r$ the recombination current density. $\gamma = 1$ if there are no leakage currents and if an exact charge balance between the two carrier types occurs; however, if all holes are used in recombinations, for example, a certain number of electrons penetrate the structure without recombination, then $\gamma < 1$. The second is the radiative singlet exciton production efficiency (η_r) due to spin statistics for production of singlet ($S = 0,\ M_s = 0$) and triplet ($S = 0,\ M_s = 1, 0, -1$) states (η_r is assumed to be 0.25). The third is the fluorescence quantum efficiency (Φ_f) which is present as non-radiative recombinations always occur (step iv′). Singlet excitons generally recombine near interfaces where quenching centres are produced, but bimolecular recombinations do not reach 100 % despite the low mobility observed in organic solids.

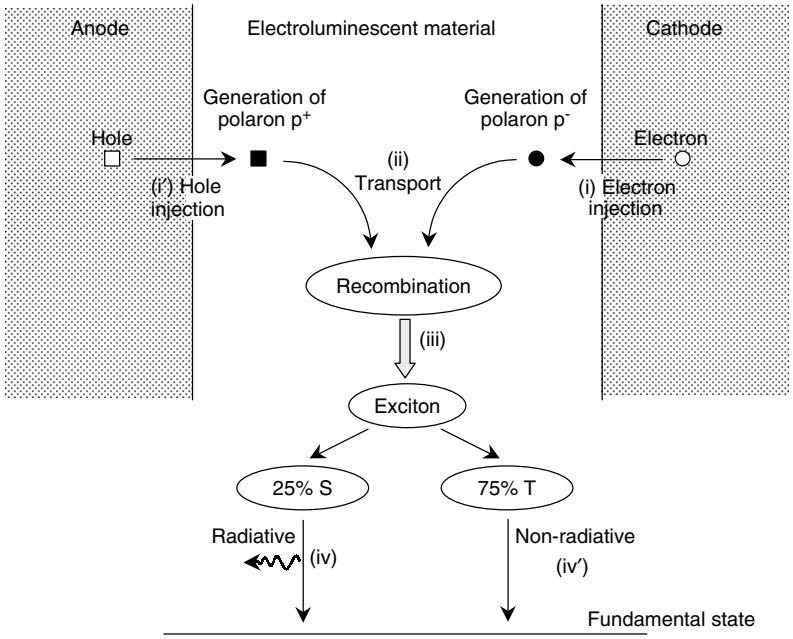

Figure 22. Successive steps to electroluminescence.

Optimisation of the quantum efficiency necessitates a variety of improvements. Firstly, the highest possible number of minority carriers undergoing radiative recombinations, which in turn requires the use of injection layers, should be attained. Given that interfaces tend to favour the presence of defects, which act as luminance extinction centres, it is judicious to move the recombination zone for the minority carriers towards the bulk of the material. This in turn necessitates the use of a minority carrier transport layer because the injection layer may not necessarily be good for minority charge transport. Secondly, the pathway for allowing emitted light to exit the device should be as efficient as possible. Thirdly, as high a level as possible of injected carrier recombination should be reached. As $\gamma = \mathcal{J}_r/\mathcal{J}_T$ will increase if $\mathcal{J}_r$ is large, the confinement zone is obtained by choosing materials which at their interfaces form barriers against holes coming from the anode and against electrons coming from the cathode. Fourthly, it is necessary to have the highest level of radiative exciton production possible. Finally, the fluorescence quantum yield (Φ_f) should be as high as possible. In addition, well-organised crystalline states and H aggregates should be avoided.

Another, delicate problem is that of ageing, which results from external effects or from the electrodes. The former may be resolved by using encapsulation, while the latter is slightly more difficult to deal with but can be resolved by using barrier layers.

POLYMERS USED IN ELECTROLUMINESCENT DEVICES

As indicated above, polymers with specific properties are chosen for particular layers.

Principal emitting polymers and adjusting emitted wavelengths

The principal emitting polymers are reported in Table 1 along with the respective λ_{max} for emitted light. The chemical formulae of the widely used poly[2-methoxy,5-(2′-ethyl-hexoxy)-1,4-phenylene vinylene] (MEH-PPV) and poly(3-octylthiophene) (P3OT) are indicated in Fig 23. The emitted wavelength can be adjusted in two ways. Firstly, as the size of the forbidden band varies with the conjugation length (n) of a polymer, when n is increased, for example by going from an oligomer to a polymer, there is a global evolution in the number of interacting states and thus a decrease in the size of the forbidden band. The result is a shift in emissions to the red. In the case of PPP, an empirical law has been given detailing the absorption peak (E_0):[33]

$$E_0 = \left[3.36 + \frac{3.16}{n}\right] \text{eV}$$, which explicitly shows that when n decreases, E_0 increases.

Table 1. The principal polymer-based emitters

Polymer	Emission λ_{max} (nm)
Fluorinated polyquinoline (PQ)	450
PPP	465
Poly(alkylfluorene)	470
Poly(3-cyclohexylthiophene) (PCHT)	555
PPV	565
MEH-PPV	605
P3OT	690

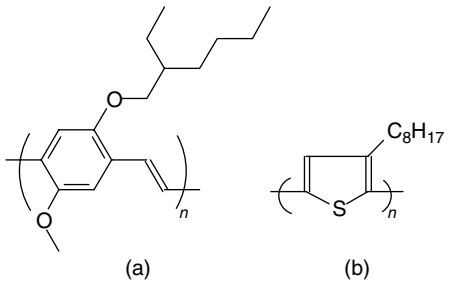

Figure 23. Chemical formulae of (a) MEH-PPV monomer unit (emission is yellow-orange) and; (b) P3OT monomer unit (emission is red).

Secondly, when monomer units within a polymer gives rise to weak π interactions (overlaps), for example between phenyl rings, the resulting gap is large. For example, PPP is a good candidate for blue emissions as its gap (emission peak at 465 nm) is greater than that of PPV (peak at 565 nm). The introduction of non-conjugated sequences, which diminish the degree of conjugation, has been used to induce a blue shift in the emission of PPV.

Polymers for hole injection layers (HILs)

To adjust the relative positions of the energy levels located at the electrode–polymer interfaces, various techniques can be used. One route is to insert a dipolar layer at the interface which induces a potential step of several tens of electronvolts. The most commonly applied method is to insert a good conducting polymer (around 10 nm thick) between electrode and emitting polymer (or the layer that transports carriers). This conducting layer generates an n^+–n or p^+–p contact. The p-type conducting poly(3,4-ethylenedioxythiophene) (PEDOT), shown in Fig 24, is very stable, exhibits a conductivity $\sigma \approx 200\,\Omega^{-1}\,\text{cm}^{-1}$ and is widely used. It acts *via*

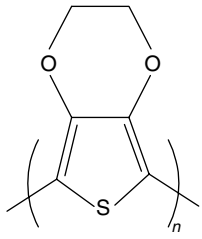

Figure 24. The repeat unit of PEDOT, which is often mixed with poly(styrene sulfonate) (PSS) to give a hole injection layer (HIL).

a 'planarisation' effect to remove defects which otherwise would prevent charge injection.[34]

Modifying polymers for use in electron transport layers (ETLs) or in hole transport layers (HTLs)

Polymer conductivities can be changed by modifying the polymer backbone with pendent electron donating or accepting groups. For the ETL, for example, the electron affinity (χ) of PPV can be increased by adding electron attracting groups, such as $-C\equiv N$, onto its backbone. Figure 25 shows the structure of CN-PPV.[35] For the HTL, the p-type character of the polymer used can be increased to improve the stabilisation of holes. This may be accomplished by introducing electron donors such as alkoxy ($-OR$) or amine ($-NH_2$) groups.[36] It is interesting to note that without modification of the chain, poly(*N*-vinyl carbazole) (PVK) (Fig 26) is intrinsically p-type[37] and that many polymers exhibit this behaviour. However, the origin of this can often be attributed to the presence of oxygen.[38]

Characterisation of multi-layer devices

Figure 27 shows the ideal scenario where all layers are involved in the electronic structure of the device. An example can be made of electroluminescent devices based on the blue emitter hexa(*para*-phenylene), commonly called parahexaphenyl. Figure 28 shows the improvement in characteristics achieved by replacing a single layer by multi-layers. A luminescence as high as 50 000 cd m^{-2} can be obtained.[39]

CHARGE GENERATION BY PHOTOEXCITATION AND THE PHOTOVOLTAIC EFFECT IN POLYMERS

General processes

In π-conjugated polymers, photon absorption results in the generation of an exciton which is an excited state. This quasi-particle diffuses inside the material as long as recombination processes (of the electron–hole pair which make up the exciton) do not take place. If the diffusion length is sufficiently long so that the exciton meets an internal field (for example, located at an acceptor–donor interface), hole and electron separation occurs and these charges are collected at their respective electrodes. If M represents the monomer of the optically excited polymer, and if z is the number of electron–hole pairs, this process is represented by $(M)_n + h\nu \rightarrow [(M)^{z+} + (M)^{z-}]_n$.

The process at a molecular scale is detailed in Fig 29, wherein we can identify: (i) the photogeneration of the exciton in the donor semiconducting polymer; (ii) the transfer of the photoinduced electron between the donor (in the excited state) and the acceptor because the LUMO level of the acceptor [typically fullerene-60 (C_{60}) or one of its derivatives] is lower than the level of the electron in the excitonic state of the donor; and (iii) the dissociation of the exciton in the donor material followed by a relaxation of charges yielding a hole in the valence band. After this process, the donor and acceptor exhibit positive and negative charges, respectively. These charges are carried through the acceptor and the

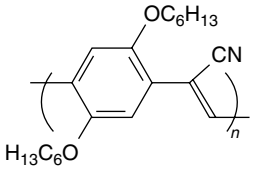

Figure 25. The repeat unit of CN-PPV.

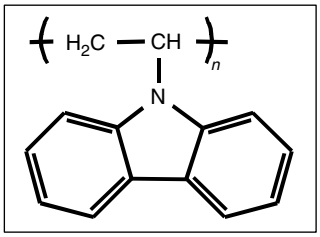

Figure 26. The repeat unit of PVK.

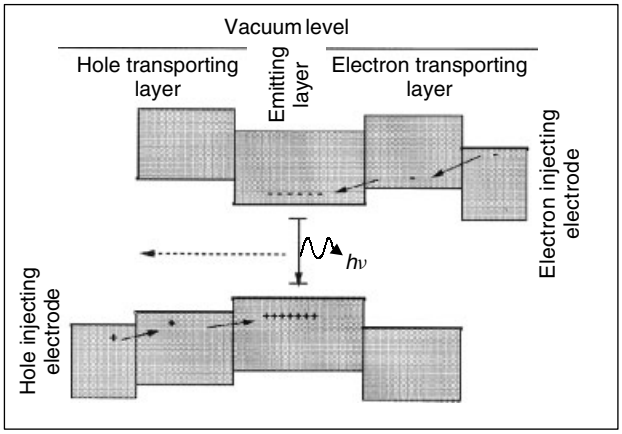

Figure 27. Schematic diagram showing improved processes in multi-layer LEDs.

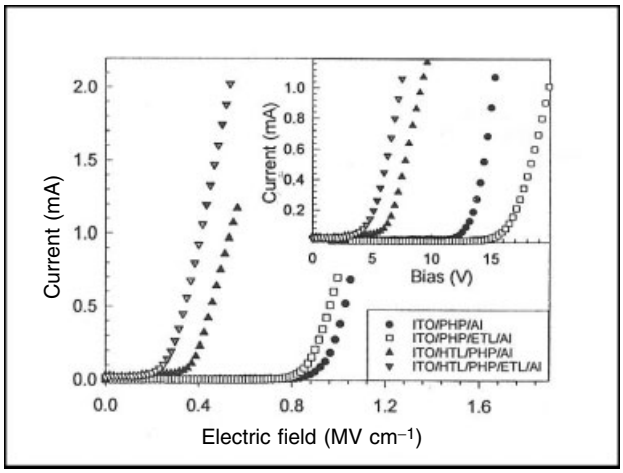

Figure 28. Current *versus* electric field characteristic for single and multi-layer electroluminescent devices; inset shows current *versus* bias voltage characteristic.

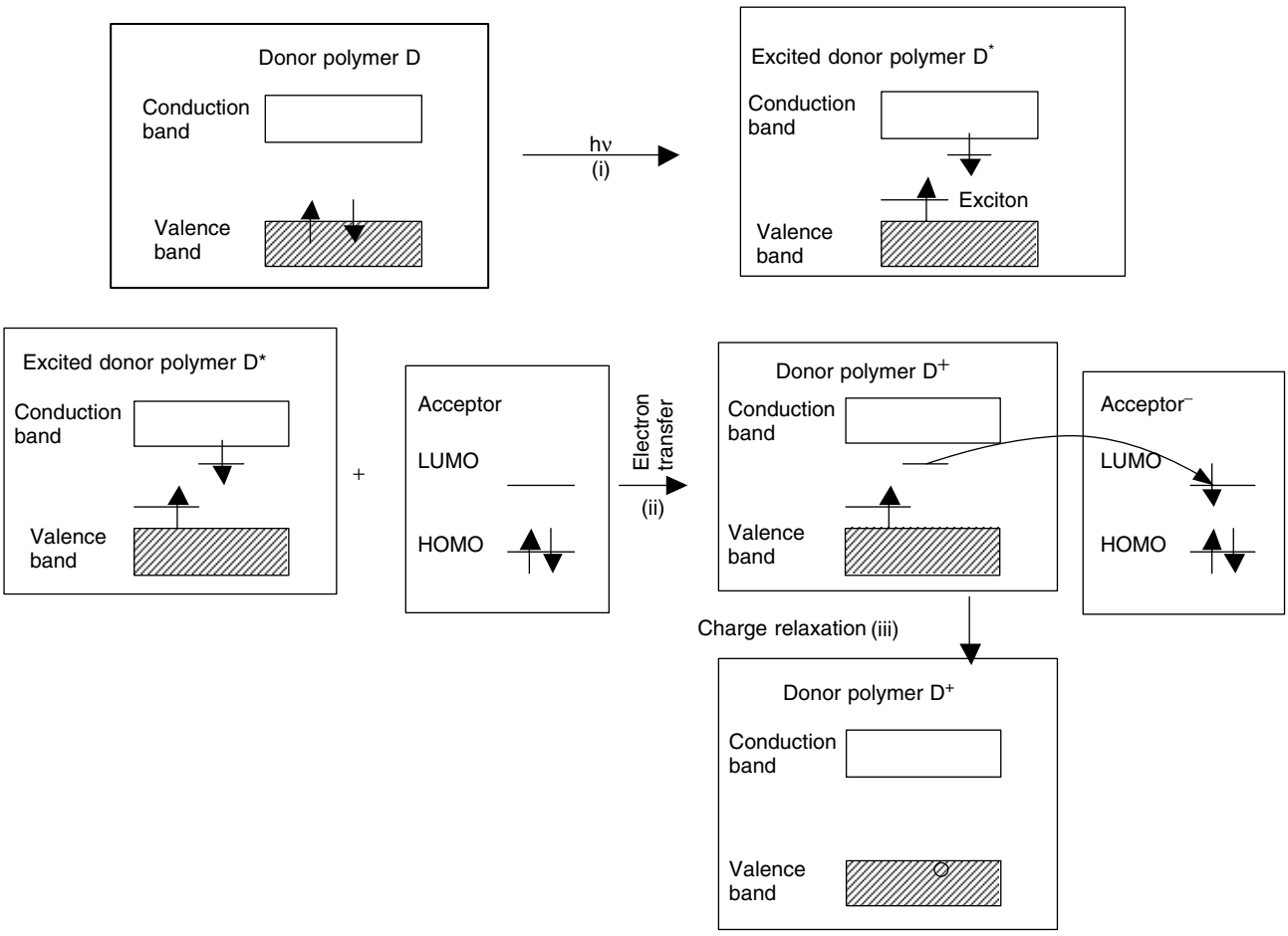

Figure 29. Schematisation of (i) exciton formation at an irradiated donor; (ii) transfer of an electron from an excited donor to an acceptor; and (iii) charge relaxation leaving a hole in the donor valence band.

donor *via* the classic transport mechanisms previously described.

Organic structures

The transfer of a photoinduced electron is allowed when the transfer time is short compared to that required for a recombination process. In addition, the LUMO level of the acceptor must be lower than the excitonic state located at the bottom of the conduction band of the donor. These conditions are simultaneously fulfilled for certain organic materials, for example, the structure MEH-PPV/C_{60}.[40] Here, the time required for charge transfer can be measured in picoseconds. Furthermore, as quantitatively shown in Fig 30, the high electron affinity of C_{60} permits facile charge transfer from the p-type MEH-PPV donor.

Classically, a photovoltaic device is made of a bilayer heterojunction. However, such a system must present some limits in performance. Even though it has a high optical absorption coefficient ($\approx 10^5$ cm^{-1}),

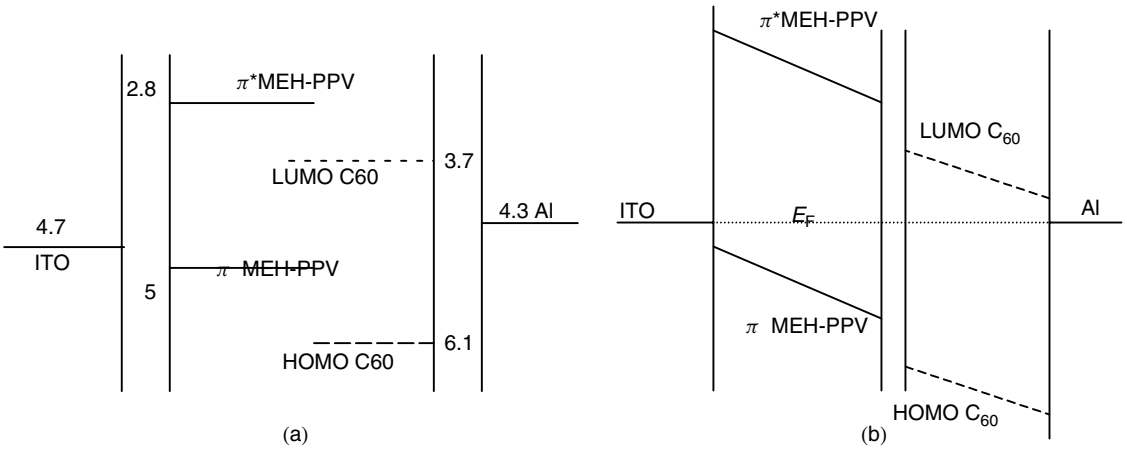

Figure 30. (a) Flat band regime of MEH-PPV/C_{60}; and (b) energy levels in MEH-PPV/C_{60} in the short-circuit state.

the absorption zone is considerably greater than the exciton diffusion length. As the exciton can only dissociate in a volume close to its zone of existence (the region at the interface between the donor polymer and the C_{60} and no further from the C_{60} than the short exciton diffusion length), all photoexcitations generated outside of this zone are condemned to undergo recombinations without generating efficiently separated carriers.

The system may be improved by using thin films of intimate mixtures of both the conjugated polymer and C_{60}. There is thus a large surface area for absorption which is always close to the polymer and C_{60} interface where the dissociation of an exciton can be assured.[41] Fig 31 shows a representation of a device made using a composite of two interpenetrating phases. The same mechanism is reproduced at each donor–acceptor element. The creation of the exciton, its dissociation, the transfer of an electron from the donor to the acceptor, and the eventual separation—in opposite directions—of the electron in the acceptor phase and of the hole in the donor phase is under the influence of the internal field generated by the asymmetric electrodes. These composite devices present a zone which is sufficiently thick to absorb light while at the same time maintaining the process of dissociation and separation of charge carriers in the volume of the layer. Outside of this, the transport mechanisms are the same as those exhibited by the bilayer device, and the mechanism used in the physical transfer of charges is the same as that schematised in Fig 32.

Under solar light, efficiencies of 3 % have been reached.[42] The composition and morphology of the film is, however, a critical factor. We should also remember that the donor–acceptor matrices should interpenetrate to a sufficient degree, so that the transport of the two charge carriers is assured. A high concentration of C_{60} can increase both the yield of carriers and their lifetimes, resulting in a global increase in current.

Alternative materials

Composite-based derivatives of PPV

The research teams of A Heeger[43] at Santa Barbara, USA, and RH Friend[44] at Cambridge, UK, independently and successfully experimented with a composite based entirely on polymers. The system used was based on MEH-PPV and CN-PPV, the former acting as donor and the latter acting as acceptor. More recent studies have resulted in even higher efficiencies by gradating the stoichiometries of the different components in the layers, facilitating conduction of electrons and holes in the volume of the heterojunction.[45]

π-Conjugated polymers grafted onto C_{60}

One way of reinforcing the contact between donor and acceptor molecules, and overcoming phase separation, is to graft the donor chain onto the acceptor. There are two notable examples: grafting PPP onto C_{60} (a route chosen by E Mignard *et al*);[46] and grafting oligo(*para*-phenylene vinylene) (OPV) onto C_{60}.[47] The structure based on 4PV is shown in Fig 33.

Using the structure ITO/C_{60}-OPV/Al (ITO stands for the transparent electrode indium tin oxide) allowed both the generation of electrons and holes and also their collection at opposing electrodes. On exposure to light, using the oligomer tri(*para*-phenylene vinylene) (3PV) an open-circuit tension of 0.46 V was obtained,

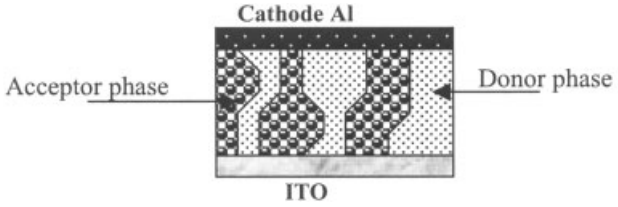

Figure 31. Schematisation of an interpenetrating structure.

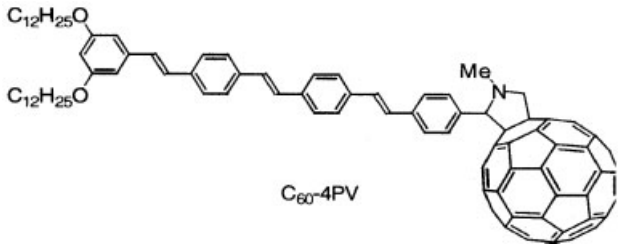

Figure 33. C_{60}-4PV.

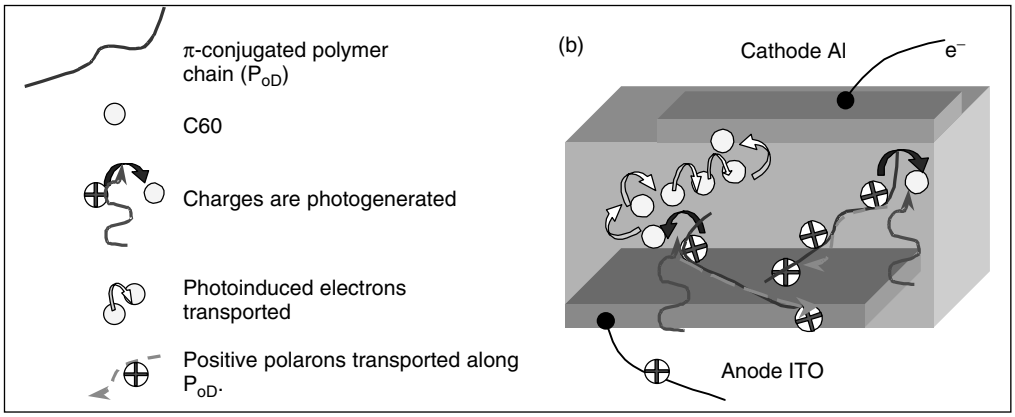

Figure 32. Schematisation of the photovoltaic process within a composite of donor polymer (P_{OD}) and C_{60}.

roughly equivalent to the difference in work functions of the ITO and Al. Under short-circuit conditions, the photo-current was found to be $10\,\mu A\,cm^{-2}$ and a fill factor (*ff*), which gives an indication of a device's internal resistance and its deviation from ideal characteristics,[48] equal to 0.3.

Materials with oriented structures

Perylene is classic n-type (acceptor) material. It is a polycyclic hydrocarbon with the chemical formula $C_{20}H_{12}$ and is used in the preparation of dyes. The structure of dipentyl perylene is shown in Fig 34(a), while another derivative of the perylene, PTCTE, is shown in Fig 34(b).

There are alternative molecules currently under study as p-type (donor) materials. They are formed by a planar, stiff, central zone connected to external chains in a star-like structure. These materials can be considered discotic, in that the disks can be piled to give columns. The structures exhibit an improved excitonic mobility leading to an increase in quantum efficiencies. Furthermore, interactions with incident light and the subsequent exciton generation are increased. Figure 35(a) shows the system denoted T_6O_2 which is a triphenylene derivative surrounded by alkoxy chains. Figure 35(b) shows a molecule studied at the Université d'Angers, France, in which the stiff central trithienobenzene group is in turn connected to three linear oligothiophene chains.[49]

The photovoltaic cell ITO/T_6O_2/perylene derivative/Al gave respectable results with $I_{short-circuit} = 46\,\mu A\,cm^{-2}$, $V_{open-circuit} = 0.7\,V$ and $ff = 0.39$.[50] The photovoltaic cell ITO/PEDOT/trithienobenzene derivative/perylene derivative/LiF/Al gave $I_{short-circuit} = 1.35\,mA\,cm^{-2}$, $V_{open-circuit} = 0.85\,V$ and $ff = 0.8$; the overall conversion factor was around 1 %.

Improving organic photovoltaic cells

Improving the photovoltaic properties of materials may require several different parameters to be dealt with. They may include: adapting the band gap of materials to solar light; orientating chromophores to generate an internal field; varying deposition techniques to increase absorption capacities; increasing charge transport capabilities; and optimisation of the morphologies. On bringing together various possible techniques, which are not necessarily mutually exclusive, the short- to medium-term aim is to realise structures which display efficiencies of the order of 5 % (a result already claimed by C Brabec at Siemens with PPV and fullerene derivatives[51]) and have lifetimes of around 5000 h.

CONCLUSION

With two types of optoelectronic systems (PLEDs and photovoltaic cells), we have shown how π-conjugated polymers offer many possibilities to realise and improve upon devices conventionally made from inorganic materials. It should be noted though that these polymers are not limited to such systems and that they may be widely applied to other domains. An

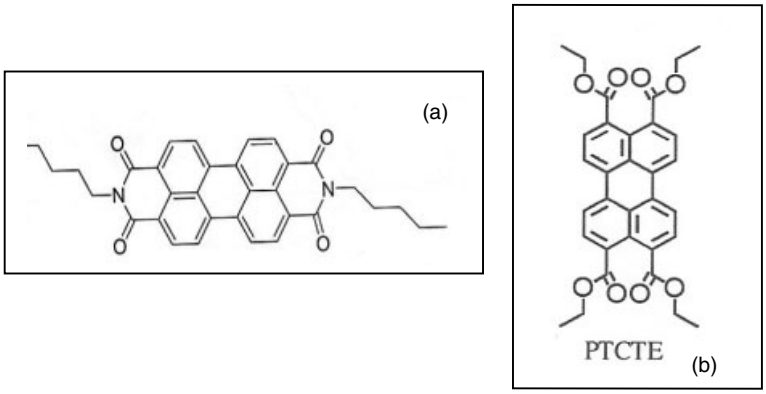

Figure 34. (a) Dipentyl perylene; and (b) PTCTE.

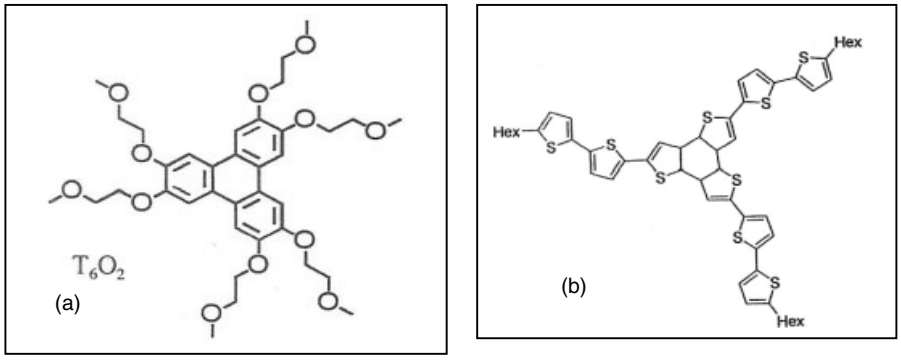

Figure 35. (a) T_6O_2 (triphenylene derivative); and (b) trithienobenzene derivative.

example is that of optoelectronic modulators,[52] devices which are important to the telecommunications industry.

It is highly probable that in the not too distant future we will see large-scale display screens and photovoltaic devices, both portable and fixed, based on these materials. Beyond the electronic properties of π-conjugated polymers, it is their good mechanical properties which will no doubt facilitate their widespread use. While the development and understanding of π-conjugated polymers has provided the impetus for their use in optoelectronics, it is now optoelectronic applications which are often providing the drive for the development of new and modified π-conjugated polymers. We have only opened a small window on what could be a very large project indeed.

REFERENCES

1 Moliton A, *Optoélectronique moléculaire et polymère: des concepts aux composants*, Springer-Verlag France and France Télécom R&D, Paris (2003). English edition, *Optoelectronics of Molecules and Polymers: from Concepts to Components*, to be published by Springer-Verlag New York in preparation.
2 Patil AO, Heeger AJ and Wudl F, *Chem Rev* **88**:183 (1988).
3 Shirakawa H, Louis EJ, MacDiarmid AG, Chiang CK and Heeger AJ, *J Chem Soc, Chem Commun* 578 (1977).
4 Heeger AJ, *Angew Chem Int Ed* **40**:2591 (2001).
5 Grem G and Leising G, *Synth Met* **57**:4105 (1993).
6 Yu G and Heeger AJ, *J Appl Phys* **78**:4510 (1995).
7 Han MG and Im SS, *J Appl Polym Sci* **71**:2169 (1999).
8 Brabec CJ, Sariciftci NS and Hummelen JC, *Adv Funct Mater* **11**:15 (2001).
9 *Handbook of Conducting Polymers*, ed by Skotheim TA, Dekker, New York (1986).
10 Peierls RE, *Quantum Theory of Solids*, Oxford University Press, London (1955).
11 Ashcroft NW and Mermin ND, *Solid State Physics*, HRW International Editions, Saunders College Publishing, Philadelphia (1976).
12 Smith RA, *Wave Mechanics of Crystalline Solids*, Chapman and Hall, London (1963).
13 Ioffe AF and Regel AR, *Noncrystalline, Amorphous and Liquid Electronic Semiconductors*, Progress in Semiconductors, Vol 4, Heywood and Co Ltd, London (1960).
14 Zuppiroli L, Bussac MN, Paschen S, Chauvet O and Forro L, *Phys Rev B* **50**:5196 (1994).
15 Gomes da Costa P, Dandrea RG and Conwell EM, *Phys Rev* **47**:1800 (1993).
16 Moliton A, Ion implantation doping of electroactive polymers and device fabrication, in *Handbook of Conducting Polymers*, ed by Skotheim TA, Dekker, New York (1998).
17 Brédas JL, Chance RR and Silbey R, *Phys Rev B* **26**:5843 (1982).
18 Brédas JL, Chance RR, Silbey R, Nicolas G and Durand P, *J Chem Phys* **77**:371 (1982).
19 Brédas JL, Chance RR and Baughman RH, *Int J Quantum Chem* **S15**:231 (1981).
20 Epstein AJ, in *Organic Electronic Materials*, ed by Farchioni R and Grosso G, *Springer Series in Material Sciences*, Springer Verlag, Berlin, p 3–37 (2001); Stejskal J and Sapurina I, *J Colloid Interface Sci* **274**(2):489–495 (2004).
21 Mott NF and Davis EA, *Electronic Processes in Non-crystalline Materials*, 2nd edn, Clarendon Press, Oxford, England (1979).
22 Kaiser AB, *Phys Rev B* **40**:2806 (1989).
23 Moreau C, Antony R, Moliton A and François B, *Adv Mat Opt Electron* **7**:281 (1997).
24 Zuppiroli L, Bussac MN, Paschen S, Chauvet O, Forro L, Bujard P, Kai K and Wernet W, Hopping in Conducting Polymers, *Proceedings of the 5th International Conference on Hopping and Related Phenomena*, ed by Addkins CJ, Long AR and McInnes JA, World of Information, Glasgow (1994).
25 Kivelson S and Heeger AJ, *Synth Met* **22**:371 (1988).
26 Brédas JL, Chance RR, Silbey R, Nicolas G and Durand P, *Phys Rev B* **26**:371 (1982).
27 Greenham NC and Friend RH, *Semiconductor Device Physics of Conjugated Polymers*, ed by Ehrenheich H, Academic Press (1996).
28 Kao KC and Hwang W, *Electrical Transport in Solids*, Pergamon Press (1981).
29 Schmidt-Mende L, Fechtenkötter A, Müllen K, Moons E, Friend RH and MacKenzie JD, *Science* **293**:1119 (2001).
30 Hamer PJ, Pichler K, Harisson MG, Friend RH, Ratier B, Moliton A, Moratti SC and Holmes AB, *Philos Mag B* **73**:367 (1996).
31 Hayachi S, Kaneto K and Yoshino K, *Solid State Commun* **61**:249 (1987).
32 Bradley DDC, *Curr Opin Solid State Mater Sci* **1**:789 (1996).
33 Leising G, Tasch S and Graupner W, Fundamentals of electroluminescence in *para*-phenylene type conjugated polymers and oligomers, in *Handbook of Conducting Polymers*, ed by Skotheim TA, Dekker, New York (1998).
34 Dietrich M, Heinze J, Heywang G and Jonas F, *J Electroanal Chem* **369**:87 (1994).
35 Friend RH, Gymer RW, Holmes AB, Burroughes JH, Marks RN, Taliani C, Bradley DDC, dos Santos DA, Brédas JL, Lögdlund M and Salaneck WR, *Nature* **397**:121 (1999).
36 Chua BS, Cacialli F, Davises JE, Feeder N, Friend RH, Holmes AB, Marseglia EA, Moratti SC, Brédas J-L and dos Santos DA, *Mat Res Soc Symp Proc: Symposium L* **488**:87 (1998).
37 Qin DS, Li DC, Wang Y, Zhang JD, Xie ZY, Wang G, Wang LX and Yan DH, *Appl Phys Lett* **78**:437 (2001).
38 Greenham NC, Friend RH and Bradley DDC, *Adv Mater* **6**:491 (1994).
39 Winkler B, Meghdadi F, Tasch S, Evers B, Schneider I, Fischer W, Stelzer F and Leising G, *Synth Met* **102**:1083 (1999).
40 Sariciftci NS, Braun D, Zhang C, Srdanov V, Heeger AJ, Stucky G and Wudl F, *Appl Phys Lett* **62**:585 (1993).
41 van Hutten PF and Hadziioannou G, The role of interfaces in photovoltaic devices, in *Molecular Materials and Functional Polymers*, ed by Blau WJ, Lianos P and Schubert U, Springer, Wien, New York (2001).
42 Brabec CJ, Sariciftci NS and Hummelen JC, *Adv Funct Mater* **11**:15 (2001).
43 Yu G and Heeger AJ, *J Appl Phys* **78**:4510 (1995).
44 Halls JJM, Walsh CA, Greenham NC, Marseglia EA, Friend RH, Moratti SC and Holmes AB, *Nature* **376**:498 (1995).
45 Brabec CJ and Sariciftci NS, Recent developments in conjugated polymer based plastic solar cells, in *Electroactive Materials*, ed by Besenhard JO, Sitte W, Stelzer F and Gamsjäger H, Springer, Vienna (2001).
46 Mignard E, Hiorns RC and François B, *Macromolecules* **35**:6132–6141 (2002).
47 Nierengarten JF, Eckert JF, Nicoud JF, Ouali L, Krasnikov V and Hadziioannou G, *Materials Today* **4**:16 (2001).
48 *ff* Is defined by the ratio of $V_{mp}I_{mp}/V_{oc}I_{sc}$, in which $V_{mp}I_{mp}$ are, respectively, tension and current at the maximum power point, V_{oc} the open-circuit tension and I_{sc} the short-circuit current.
49 Bettignies R, *Cellules photovoltaïques organiques dérivées de nouveaux systèmes conjugués*, PhD thesis no 573, Université d'Angers, France (2003).
50 Oukachmih M, *Les cellules photovoltaïques à base de matériaux organiques dicotiques*, PhD thesis, Université de Toulouse, France (2003).
51 Boulben A, Les cellules solaires organiques atteignent 5 % de rendement, *L'Usine nouvelle*, **2901**:37 (2004).
52 Donval A, Toussaere E and Hierle R, Zyss J, *J Appl Phys* **87**:3258–3262 (2000).